2010 IEEE International Conference on Robotics and Automation
Anchorage Convention District
May 3-8, 2010, Anchorage, Alaska, USA

A Digital Input Shaper for Stable and Transparent Haptic Interaction

Yo-An Lim and Jeha Ryu
Department of Mechatronics, Gwangju Institute of Science and Technology (GIST)
1, Oryong-dong, Buk-gu, Gwangju, 500-712, Korea
yo-anl@gist.ac.kr, ryu@gist.ac.kr

Abstract— **This paper presents a frequency-dependent digital damping referred to a digital input shaper (DIS). Compared to the previously proposed analog input shaper, the DIS makes the implementation of damping much more flexible and significantly reduces the electrical noise. Moreover, the DIS can incorporate position control at the initial contact with virtual objects to improve the perceived contact hardness. Through benchmark virtual wall experiments, we show that the DIS can significantly increase the impedance range that a haptic interface can stably display, and that the initial contact hardness that a user perceives can be noticeably improved by using the proposed position control method.**

I. Introduction

Haptic interfaces provide users with a sense of touch in response to their hand movements in virtual or real environments. Ideally, haptic interfaces should transparently display the entire impedance range of the environment they are interacting with. In practice, however, the impedance range that a haptic interface can stably display is limited; most notably, displaying very high stiffness is still a challenging problem.

To increase the stably displayed impedance range, a number of attempts have been made. For example, Mehling et al. [1] suggested frequency-dependent analog damping, which was installed in parallel with a motor. As another analog damping method, Weir et al. [2] implemented an analog circuit to estimate the motor back EMF that was used to determine the magnitude of the added damping. In other studies, Gosline et al. [3] proposed mechanical damping that was based on a tunable eddy current brake, and Ryu et al. [4] proposed a haptic stability controller to provide variable damping according to haptic instability analyzed by the motor motion in the frequency domain. Also, Diolaiti et al. [5] and Wilson et al. [6] exploited electrical dynamics of DC motors to display high stiffness, and Srikanth et al. [7] modified the driving signal of an H-bridge amplifier of DC motors to provide damping.

An additional method for adding frequency-dependent damping to a haptic system, referred to as an analog input shaper (AIS), was proposed in [8], [9]. However, since the AIS is composed of analog electrical circuits, the damping design is quite inflexible and it is liable to have electrical noise. Moreover, the AIS significantly deteriorates the quality of the perceived initial contact hardness due to the nature of its low-pass filter.

In this paper, therefore, we present a digital input shaper (DIS) that is a discrete-time implementation of the previously proposed AIS, which uses a digital signal processor (DSP) and a position control method to improve the perceived initial contact hardness. Virtual wall experiments show that the DIS can improve the impedance range that a haptic interface can stably display, and also that the human perception of hardness is significantly improved by using the proposed position control method.

The remainder of this paper is organized as follows. In section II, we briefly discuss the architecture and characteristics of the frequency-dependent damping added to the signal stage. In section III, the proposed DIS and a method for improving the initial contact hardness are discussed. Experiment results are shown in section IV, and finally in section V we discuss our conclusions.

II. Frequency-Dependent Damping

A haptic system is a sampled-data system that includes both continuous and discrete systems, where the sampling and sensor quantization are the main factors limiting performance, such as in the stable display of rigid virtual objects using a haptic interface. Fig. 1 shows a simplified model of a haptic system that includes a virtual environment, a human operator, and a haptic interface. In the figure, K, B, M, and F are the stiffness, damping, mass, and force, respectively; similarly, the subscripts *VE*, *H*, and d represent the virtual environment, human operator, and haptic interface.

High frequency force inputs (F_{VE}) in a haptic system can make the system unstable [1], [9], and thus adding damping elements to high frequency inputs should assist in increasing the stability of a haptic system. Fig. 2 shows a block diagram of a haptic system with the added damping element that we are interested in. In the figure, the damping element takes the force from the virtual environment as an input, and it outputs a damped force signal to a haptic interface.

The fundamental concept of the frequency-dependent damping in a haptic system is to add a low-pass filter, though the location of damping can vary, such as being placed in the signal stage [8], [9] or in the power stage [1]. Note that a more detailed comparison of frequency-dependent damping in the signal and power stages can be found in [9], and in this paper our focus is on the damping located in the signal stage as shown in Fig. 3 that illustrates frequency-dependent damping located just before the motor current amplifier. By adding a low-pass filter, as shown in the figure, the dynamic equation of the system becomes

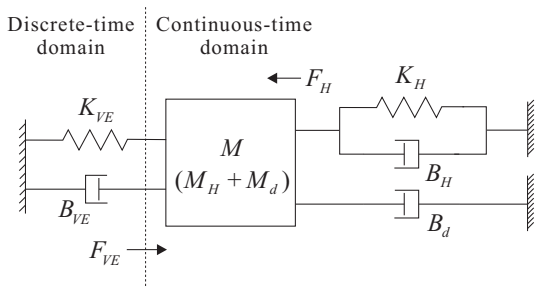

Fig. 1. Haptic system model.

$$\left[A(s)J_d s^2 + A(s)B_d s\right]\theta_d = K_t K_i V(s) \qquad (1)$$
$$A(s) = \left(1 + \frac{z_1(s)}{z_2(s)}\right)$$

where J_d, B_d, θ_d, K_t, K_i, and v represent the inertia, damping, position of haptic interface, motor torque constant, amplifier current constant, and amplifier input voltage, respectively. Then, by comparing this system to system dynamics without a low-pass filter [i.e., $\left(J_d s^2 + B_d s\right)\theta_d = K_t K_i V(s)$], it can be seen that the low-pass filter changes the system damping to $A(s)B_d$; Fig. 4(a) shows system damping when the low-pass filter is a 1st order Butterworth filter with a cutoff frequency of 2.5 Hz and B_d is 0.05 Nms/rad. As in the figure, the low-pass filter makes the damping frequency-dependent—the damping increases at higher frequencies, and decreases at lower frequencies. This frequency-dependent damping is the primary advantageous behavior of low-pass filters.

However, it should also be noted that a low-pass filter inevitably produces time-delay, known as one of the major causes of instability in haptic systems. The relationship between the input command torque (τ_{VE}) and output torque (τ_d) can be obtained as (2), and Fig. 4(b) shows the delay between them. In the figure, the delay increases as the frequency increases.

$$\frac{\tau_d(s)}{\tau_{VE}(s)} = \frac{z_2(s)}{z_1(s) + z_2(s)} \qquad (2)$$

From the above discussion, it can be seen that there is a tradeoff in adding frequency-dependent damping; the damping added to the high frequency region increases the stability of a haptic system, though the delay decreases the stability. However, although a quantitative analysis of this tradeoff is still under investigation, initial experimental results show that the benefit of adding frequency-dependent damping is larger than the loss of stability incurred by the time-delay.

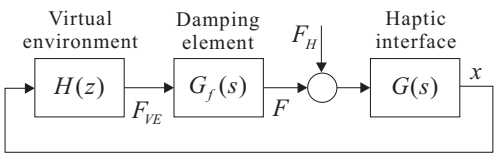

Fig. 2. Adding a damping element to a haptic system.

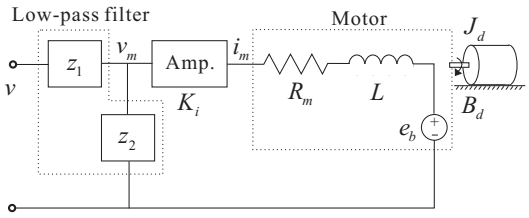

Fig. 3. Frequency-dependent damping in the signal stage.

III. Digital Input Shaper

In addition to the frequency-dependent damping in the signal stage, the AIS includes two linear half-wave rectifiers [9], as shown in Fig. 5. Note that a low-pass filter can be realized by subtracting the output of a high-pass filter from the input. A high-pass filter extracts high frequency signals from the input and the rectifiers enable a fast signal decrease, which subsequently reduces the energy generated by time-delay and the non-negative input to a haptic interface when a haptic point leaves the virtual environment [9]. However, these rectifiers also cause nonlinear characteristics in the AIS and thereby make the theoretical analysis very difficult; a detailed description and function of rectifiers can be found in [8]. In brief, the AIS is comprised of an analog high-pass filter, adders, and rectifiers that are mainly implemented using OP-amps. Thus, if we want to change the characteristics of the AIS, such as its filter cutoff frequency, filter order, or filter type, we need to modify the analog hardware, and analog circuits are apt to have electrical noises. As such, in order to solve these difficulties, i.e., for more flexibility and less noise, the DIS is implemented using a DSP.

A. Discrete-Time Implementation of AIS

Fig. 6 shows a haptic system with the proposed DIS. In order to make the discrete-time implementation behave more like its analog counterpart, the sampling rate of the DIS ($1/T_2$) is chosen to be as high as the DSP allows, which

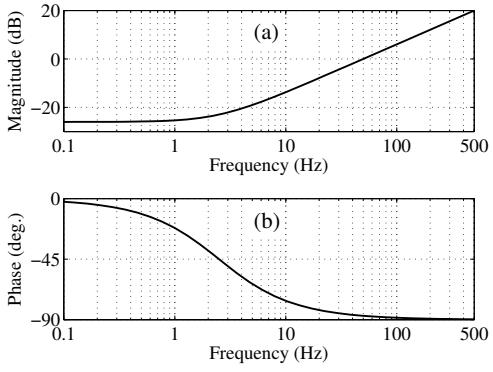

Fig. 4. (a) System damping and (b) time-delay between τ_d and τ_{VE}.

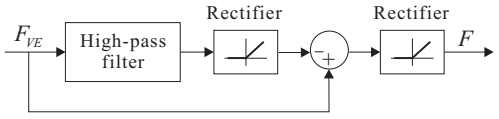

Fig. 5. Analog input shaper implemented using analog circuits.

is generally much higher than that of the haptic system controller ($1/T_1$, typically set at 1 kHz); here, $1/T_2$ is set at 100 kHz. In the current DIS, the high-pass filter is a digital Butterworth filter, and adders and rectifiers can be easily implemented through its software. In addition, parameters for various filters are stored in the DSP, and can be adaptively selected according to the specific control situations.

B. Improvement of Initial Contact Hardness

The major disadvantage of the DIS is that the initial contact hardness a user perceives is deteriorated, since it reduces the high frequency transient inputs that are very helpful in improving the realism of the contact to stiff virtual objects [10]. In order to overcome this problem, we propose a method based on position control for the short duration of initial contact. The motivation of the proposed method is that when an object collides with a very stiff object, it instantly stops upon impact. Previously, Salcudean et al. [11] applied a braking force pulse to make the velocity of a moving mass zero when crossing into a virtual wall. In their method, however, system dynamics such as inertia and velocity should be known, whereas the proposed position control method needs no prior information.

The proposed method can be summarized as in (3) and is depicted in Fig. 7.

$$\begin{aligned} F(k) &= w_1(k)F_1(k) + w_2(k)F_2(k) \qquad (3)\\ w_1(k) &= \frac{T_2}{T_p}(k-k_0)\\ w_2(k) &= \left(1-\frac{T_2}{T_p}(k-k_0)\right) \end{aligned}$$

Here, $F_1(k)$, $F_2(k)$, $w_1(k)$, $w_2(k)$, and k_0 are the output of the DIS, output of the position controller, DIS weight, position controller weight, and the control step when initial contact occurs, respectively. In addition, T_p is the position control duration, which needs to be long enough to stop the haptic point at the initial contact point using the position

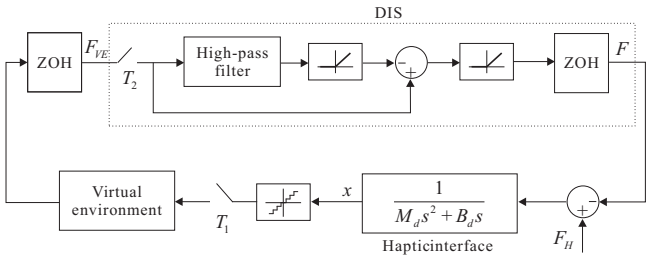

Fig. 6. Haptic system with DIS.

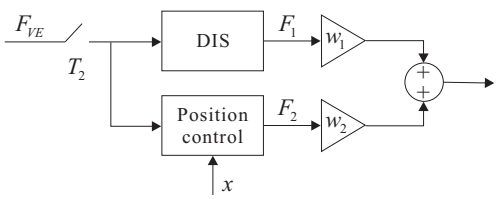

Fig. 7. Improving initial contact hardness.

control. It should also be noted, however, that if the duration is too long a user may feel a sticky force holding the haptic interface to a specific position; therefore, to prevent this situation the duration needs to be minimized. Empirical studies show that the control duration needs to be approximately tens of milliseconds, which is similar to the short-duration transient at impact that creates high-frequency acceleration and allows the user to infer material properties of the objects, as discussed in [10]. The weights w_1 and w_2 are introduced to ensure a smooth transition between the position control and DIS output, with lower and upper bounds set at 0 and 1, respectively. In this work, w_1 is 0 at the initial contact and linearly increases until reaching 1 when T_p has elapsed since the initial contact, while w_2 decreases from 1 to 0 during this same period, as shown in Fig. 8. Thus, after the position control duration, only F_1 affects the system.

The position control is implemented as

$$F_2(k) = K_p\left(x(k) - x(k_0)\right) + K_d\dot{x}(k) \qquad (4)$$

where, x is the position of the haptic interface, and K_p and K_d are the position control gains and can be thought as a proportional and a derivative gain of PID control, respectively. Then, assuming that $x(k_0)$ is the boundary of a virtual object, (4) is the same as the force calculation of haptic interaction with a virtual object that consists of stiffness and damping, except there is no unilateral constraint. Thus, when K_p and K_d are the same as the stiffness and damping of a virtual object, the user can feel the impedance of the object for a short period without losing stability. Also, note that the position control rate (100 kHz) is much higher than the haptic control rate (1 kHz), and that this higher control rate is known to be very helpful in stably displaying a higher impedance. However, the high control rate makes

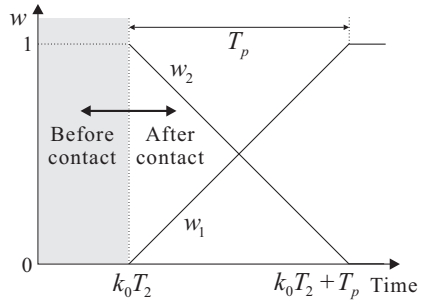

Fig. 8. Weight variations of the initial contact position control.

the granularity of velocity estimation large, especially for a haptic interface that typically moves at low velocities [12]. For better velocity estimation, methods suggested in [13], [14], and [12] can be applied, but in this paper the virtual object is assume to be a spring that needs no velocity estimation.

IV. Experiments

Through virtual wall experiments, we show that the proposed DIS can significantly increase the impedance range that a haptic interface can stably display. Moreover, it is shown that the initial contact hardness that a human user perceives can be noticeably improved by using the proposed position control method.

Fig. 9 shows the DIS and custom-built 1-DOF haptic interface used for experiments. The DIS includes a DSP module (TI, TMS320F28335), a 16-bit D/A converter, and interface circuits. In this paper, the control rate of the DSP is set to 100 kHz, and the filter in the DIS is a 1st order digital Butterworth filter having a cutoff frequency of 2 Hz. Note that since the frequency of the voluntary motion of human hands is known to be a few Hz, when designing the frequency-dependent damping it would be reasonable to select a cutoff frequency within this range. The custom-built haptic interface consists of a brushed DC motor (Maxon RE30) and an encoder having a resolution of 8000 pulses/rev, and the motor torque is amplified twelve times using a capstan mechanism.

As benchmark tests, virtual wall experiments are performed for various virtual stiffnesses, and a method for improving the initial contact hardness is also tested. For experimental consistency, we attempted to maintain the same approach velocity and grip condition during every trial.

A. Virtual Wall Experiments

First, virtual wall experiments were conducted without the DIS for various virtual stiffnesses (K_{VE}). Note that the results shown in Figs. 10 and 11 are not forces exerted at the human hand, but are the command forces at the current amplifier input; when the DIS is not used the force is from a controller (F_{VE}), and when the DIS is used the force is the output of the DIS (F). Note also that the force exerted at the human hand can be analytically calculated or can be directly measured using a force sensor. Also, the virtual wall is located at 0.1 m.

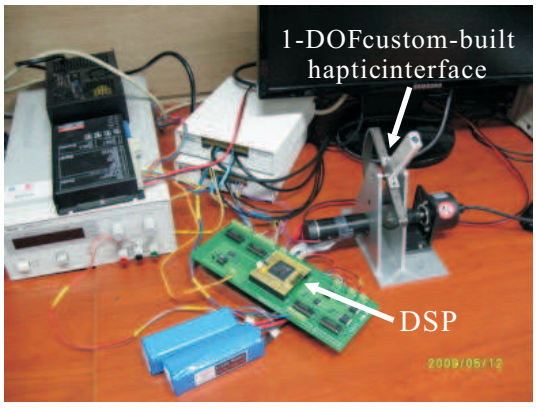

Fig. 9. Experimental setup: DIS and 1-DOF haptic interface.

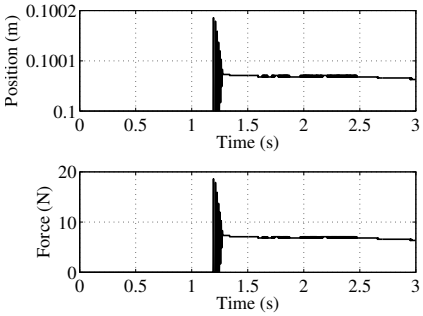

(a) $K_{VE} = 100$ kN/m

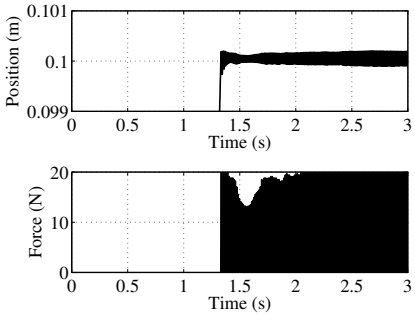

(b) $K_{VE} = 120$ kN/m

Fig. 10. Experimental results without DIS.

Figs. 10(a) and 10(b) show the experimental results for virtual stiffnesses of 100 kN/m and 120 kN/m, respectively. The figures show that when the DIS is not used, the interaction becomes unstable when K_{VE} is approximately 120 kN/m. Conversely, when the DIS is used the interaction becomes unstable at approximately 220 kN/m, as shown in Figs. 11(a) and 11(b). In Figs. 10(a) and 11(a), the force magnitudes are almost same in steady-states, whereas the penetration depth in Fig. 10(a) is almost twice of that in Fig. 11(a). Therefore, these results confirm that the DIS can significantly increase the stiffness range (approximately two times from 100 kN/m to 200 kN/m) that a haptic interface can stably display. Note, however, that the performance improvement when using the DIS can vary for different haptic interfaces, as reported in [9].

B. Initial Contact Hardness

As previously discussed, the DIS reduces the high frequency transient inputs, thereby deteriorating the initial contact hardness that a human user perceives. Fig. 12 shows the displayed stiffness of the experiments in Fig. 11(a). As shown in the magnified plot, the increase of the displayed stiffness at initial contact is relatively slow, which makes a user feel less stiff virtual wall. To improve the initial contact hardness, the position control method at the initial contact discussed above

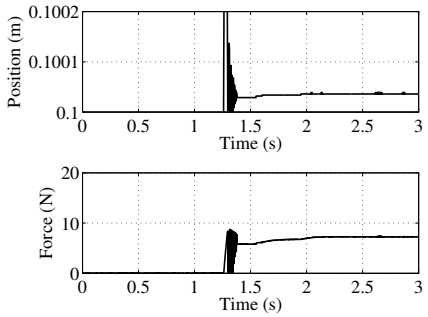

(a) $K_{VE} = 200$ kN/m

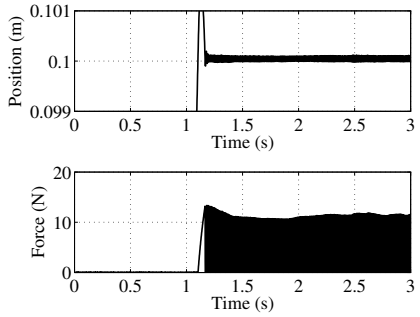

(b) $K_{VE} = 220$ kN/m

Fig. 11. Experimental results with DIS.

is applied. To this end, Figs. 13 and 14 respectively show the experimental results and the displayed stiffness when the proposed method is used, where the position control duration (T_p) is set at 100 ms. From the figures, a fast increase of the displayed stiffness at initial contact can be observed, while stability is maintained. Then, in order to ensure that a user really feels a higher initial contact hardness with the proposed method, a performance metric linked to human perception of hardness, referred to as rate hardness [15], is considered. The rate hardness is defined as below.

$$\text{Rate hardness} = \frac{\text{initial force rate of change (N/s)}}{\text{initial penetration velocity (m/s)}}$$

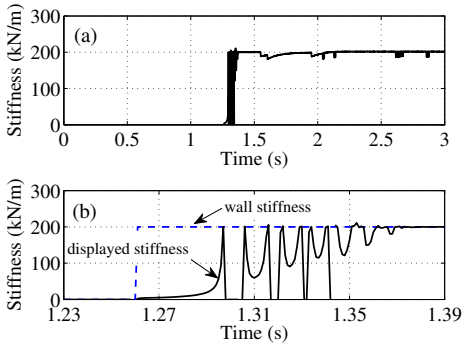

Fig. 12. Displayed stiffness (a) without initial contact position control and (b) its magnified plot when $K_{VE} = 200$ kN/m.

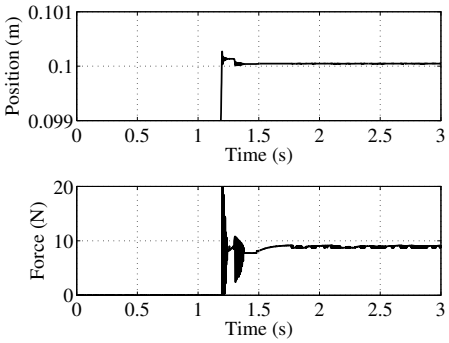

Fig. 13. Experimental results with DIS and initial contact position control ($K_{VE} = 200$ kN/m).

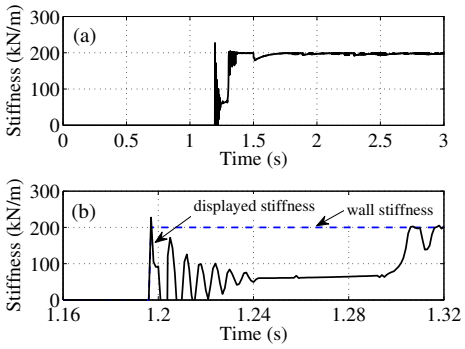

Fig. 14. Displayed stiffness with (a) initial contact position control and (b) its magnified plot when $K_{VE} = 200$ kN/m.

Fig. 15 shows the mean and standard deviation of the rate hardness obtained from 30 virtual wall experiments at the stiffness of 200 kN/m. As seen in the figure, when the proposed position control method is used, the rate hardness becomes much higher (approximately 180 times), which leads to higher hardness perception. It should be noted, however, that when position control at the initial contact is applied, there is a unnatural change in the displayed stiffness just after the end of the position control—this occurrence is still under investigation.

V. Conclusions

In this paper, a frequency-dependent damping element referred to a digital input shaper (DIS) is presented, and a method for overcoming the degradation of initial contact hardness, a major disadvantage of the DIS, is proposed. Through virtual wall experiments, we show that the DIS can significantly increase the stably displayed impedance range. In addition, it was found that the position control method at the initial contact can significantly improve the human perception of hardness without losing stability.

Acknowledgments

This research was supported by the MKE (The Ministry of Knowledge Economy), Korea, under the ITRC (Information

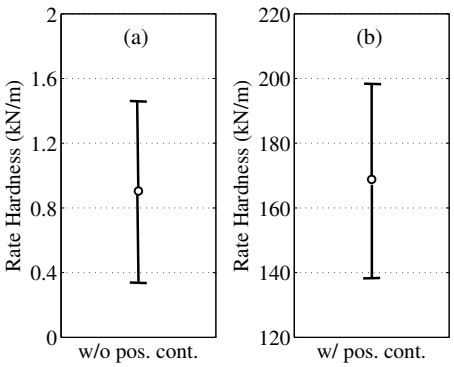

Fig. 15. Rate hardness (a) without initial contact position control and (b) with initial contact position control when $K_{VE} = 200$ kN/m.

Technology Research Center) support program supervised by the NIPA (National IT Industry Promotion Agency) (NIPA-2009-C1090-0902-0008), and by the Ministry of Culture, Sports and Tourism (MCST) and Korea Creative Content Agency (KOCCA) in the Culture Technology (CT) Research and Development Program 2009.

REFERENCES

[1] J. S. Mehling, J. E. Colgate, and M. A. Peshkin, "Increasing the impedance range of a haptic display by adding electrical damping," in *Proceedings of the First Joint Eurohaptics Conference and Symposium on Haptic Interfaces for Virtual Environment and Teleoperator Systems*, March 2005, pp. 257–262.

[2] D. W. Weir, J. E. Colgate, and M. A. Peshkin, "Measuring and increasing z-width with active electrical damping," in *Proceedings of the Symposium on Haptic Interfaces for Virtual Environments and Teleoperators Systems 2008*, Reno, Nevada, USA, March 2008, pp. 169–175.

[3] A. H. Gosline, G. Campion, and V. Hayward, "On the use of eddy current brakes as tunable, fast turn-on viscous dampers for haptic rendering," in *Proceedings of Eurohaptics*, 2006, pp. 229–234.

[4] D. Ryu, J.-B. Song, S. Kang, and M. Kim, "Frequency domain stability observer and active damping control for stable haptic interaction," *IET Control theory and Applications*, vol. 2, no. 4, pp. 261–268, 2008.

[5] N. Diolaiti, G. Niemeyer, and N. A. Tanner, "Wave haptics: Building stiff controllers from the natural motor dynamics," *Int. J. Rob. Res.*, vol. 26, no. 1, pp. 5–21, 2007.

[6] R. Wilson and G. Niemeyer, "Motion control of impedance-type haptic devices," in *Proceedings of the 2009 IEEE International Conference on Robotics and Automation*, 2009, pp. 1092–1097.

[7] M. B. Srikanth, H. Vasudevan, and M. Muniyandi, "DC motor damping: A strategy to increase passive stiffness of haptic devices," in *Haptics: Perception, Devices and Scenarios*, ser. LNCS, M. Ferre, Ed., vol. 5024. Springer, 2008, pp. 53–62.

[8] Y.-A. Lim, H. S. Ahn, and J. Ryu, "Performance of equivalent frequency-dependent damping," in *Proceedings of World Haptics 2009 (The Third Joint Eurohaptics Conference and Symposium on Haptic Interfaces for Virtual Environment and Teleoperator Systems)*, Salt Lake City, UT, USA, March 2009, pp. 559–564.

[9] Y.-A. Lim, H.-S. Ahn, and J. Ryu, "Analogue input shaper for haptic interfaces," *IET, Control Theory and Applications*, vol. 3(12), pp. 1553–1564, 2009.

[10] K. J. Kuchenbecker, J. Fiene, and G. Niemeyer, "Improving contact realism through event-based haptic feedback," *IEEE Transactions on Visualization and Computer Graphics*, vol. 12, no. 2, pp. 219–230, 2006.

[11] S. E. Salcudean and T. D. Vlaar, "On the emulation of stiff walls and static friction with a magnetically levitated input/output device," *Journal of Dynamic Systems, Measurement, and Control*, vol. 119, pp. 127–132, 1997.

[12] M. C. Cavusoglu, D. Feygin, and F. Tendick, "A critical study of the mechanical and electrical properties of the phantom haptic interface and improvements for high-performance control," *Presence*, vol. 11, no. 6, pp. 555–568, 2002.

[13] J. E. Colgate and J. M. Brown, "Factors affecting the Z-Width of a haptic display," in *Proceedings of the IEEE 1994 International Conference on Robotics and Automation*, San Diego, CA, May 1994, pp. 3205–3210.

[14] F. Janabi-Sharifi, V. Hayward, and C.-S. J. Chen, "Discrete-time adaptive windowing for velocity estimation," *IEEE Transactions on Control Systems Technology*, vol. 8, no. 6, pp. 1003–1009, 2000.

[15] D. A. Lawrence, L. Y. Pao, A. M. Dougherty, M. A. Salada, and Y. Pavlou, "Rate-hardness: A new performance metric for haptic interfaces," *IEEE Transactions on Robotics and Automation*, vol. 16, no. 4, pp. 357–371, 2000.